Talanta 130 (2014) 55–62

Contents lists available at ScienceDirect

Talanta

journal homepage: www.elsevier.com/locate/talanta

Photochemical decoration of magnetic composites with silver nanostructures for determination of creatinine in urine by surface-enhanced Raman spectroscopy

Melisew Tadele Alula, Jyisy Yang *

Department of Chemistry, National Chung-Hsing University, Taichung 402, Taiwan

ARTICLE INFO

Article history:
Received 16 January 2014
Received in revised form
19 June 2014
Accepted 20 June 2014
Available online 30 June 2014

Keywords:
Creatinine
Magnetic particles
Photoreduction
Silver nanoparticles
Surface-enhanced Raman scattering
ZnO

ABSTRACT

In this study, silver nanostructures decorated magnetic nanoparticles for surface-enhanced Raman scattering (SERS) measurements were prepared via photoreduction utilizing the catalytic activity of ZnO nanostructure. The ZnO/Fe_3O_4 composite was first prepared by dispersing pre-formed magnetic nanoparticles into alkaline zinc nitrate solutions. After annealing of the precipitates, the formed ZnO/Fe_3O_4 composites were successfully decorated with silver nanostructures by soaking the composites into silver nitrate/ethylene glycol solution following UV irradiations. To find the optimal condition when preparing Ag@ZnO/Fe_3O_4 composites for SERS measurements, factors such as the reaction conditions, photoreduction time, concentration of zinc nitrate and silver nitrate were studied. Results indicated that the photoreduction efficiency was significantly improved with the assistance of ZnO but the amount of ZnO in the composite is not critical. The concentration of silver nitrate and UV irradiation time affected the morphologies of the formed composites and optimal condition in preparation of the composites for SERS measurement was found using 20 mM of silver nitrate with an irradiation time of 90 min. Under the optimized condition, the obtained SERS intensities were highly reproducible with a SERS enhancement factor in the order of 7. Quantitative analyses showed that a linear range up to 1 μM with a detection limit lower than 0.1 μM in the detection of creatinine in aqueous solution could be obtained. Successful applying of these prepared composites to determine creatinine in urine sample was obtained.

1. Introduction

Creatinine is a metabolite of creatine and is eliminated from the human body through urinary excretion [1]. The concentration of creatinine in urine and serum can reveal the status of renal, muscular, and thyroid functions [2–6]. It also serves as a marker of metabolic abnormalities, neuroendocrine activation, and vascular diseases [7]. A large number of methods have been proposed to analyze the levels of creatinine in urine samples, including enzyme-based colorimetric [8–11], chromatographic [12,13], electrochemical methods [14,15] and others [16–18]. These methods generally suffer in one of the weakness such as tiresome sample preparation steps, complicated reagents, skillful operators, and interferences from drug and indigenous species from biological fluids. On the other hand, surface-enhanced Raman spectroscopy (SERS) has gained much attention in recent years owing to its potential to be an extremely sensitive means for analytical applications [19–21]. The treatment of creatinine sample is largely simplified in SERS type of measurements while promising results have been obtained in the analyses of creatinine in urine [22–25]. For example, Premasiri et al. [22] studied the potential of the SERS method for analyzing creatinine in artificial urine using gold colloids as the SERS active substrate. Gold colloids have been prepared and used alone [23] or decorated on nanostructured poly(chloro-p-xylene) [24] for quantitatively analyzing the creatinine level in urine. However, due to the small cross section of creatinine in Raman measurements, a highly sensitive SERS active substrate is essentially needed to enlarge the analytical signals. By improving the sensitivity in SERS measurements, the strong interferences from the urine sample can be largely reduced by a dilution method, which is a common method used for analytical technique with enough sensitivity. Therefore, to improve the sensitivity and to minimize the steps in the preparation of highly sensitive SERS substrates, a photochemical method to prepare composite composed of silver, ZnO and magnetic nanostructure is proposed in this work and targeted for sensitive detection of creatinine in urine samples by SERS.

Multifunctional hybrid structures have received great attention because these composites exhibit properties that would not have been obtained only from a single component counterpart. Among the various functional nanomaterials, ZnO-based hybrid materials containing silver give rise to a significant local field amplification

* Corresponding author. Tel.: +886 422840411x514; fax: +886 422862547.
E-mail address: jyisy@dragon.nchu.edu.tw (J. Yang).

http://dx.doi.org/10.1016/j.talanta.2014.06.047
0039-9140/

that results from the accumulated electrons created by Ag/ZnO heterojunction [26,27]. This property makes the Ag/ZnO composites applicable in the field of SERS measurements [27–31]. Isolation and recovery of the Ag/ZnO (or Au/ZnO) composite with the adsorbed analyte's molecules from the aqueous suspension for SERS measurement, however, are not easy [26,32]. Tiresome procedure to deposit metal nanoparticles onto ZnO using linker agents that may compromise the cleanliness of the substrate for SERS measurement is an additional problem [33,34]. Moreover, accessibility of ZnO nanorods for uniform deposition of Ag nanostructures is challenging [35]. Here, these difficulties are circumvented by introducing magnetic particles as a platform for the Ag/ZnO hybrid structure where the composites are readily collected from the reaction mixture using an external magnet that needs no centrifugation or filtration. Most importantly, the enrichment effect acquired from the magnetic property of the composite is intensively pronounced and helps decrease the detection limit by using a small amount of Ag nanostructures-decorated magnetic particles, which allows complete saturation of a low concentration of analytes that enables detection of a minute amount of analytes.

In this work, ZnO is initially incorporated into magnetic nanoparticles to render magnetic and photocatalytic properties for the composite. UV light exposure of the mixture containing $AgNO_3$ solution (dissolved in ethylene glycol) and ZnO/Fe_3O_4 composite resulted in the formation of silver nanostructures onto the composite. Therefore, the composite exhibits a multifunctional advantage of optical, magnetic and photocatalytic properties given by the nanostructures of Ag, Fe_3O_4 and ZnO, respectively. The schematic diagram for the preparation of the hybrid structures in this work is shown in Fig. 1a. As can be seen in this diagram, the magnetic particles of Fe_3O_4 are first prepared from coprecipitation of Fe (II) and Fe (III) with a hydroxide solution. By dispersing magnetic particles into zinc nitrate solution, a hydroxide solution is used to form precipitates of $Zn(OH)_2$ on the magnetic particles. After annealing, ZnO/Fe_3O_4 composites were formed. By soaking ZnO/Fe_3O_4 composites into silver nitrate/ethylene glycol solution, Ag nanostructures-decorated ZnO/Fe_3O_4 composites with high SERS effect are formed. A series of pictures taken in each of the above steps is also plotted in Fig. 1b for reference.

2. Experimental

2.1. Chemicals

Iron (II) sulfate heptahydrate, iron (III) sulfate n-hydrate and sodium hydroxide were obtained from Showa (Tokyo, Japan). Ammonium hydroxide (28–30% (w/v)) was purchased from Acros (Phillipsburg, NJ, USA). *p*-Nitrothiophenol (pNTP) was obtained from TCI (Tokyo, Japan). Methanol was obtained from Echo chemical (Toufen, Taiwan). Silver nitrate was purchased from J.T. Baker (Phillipsburg, NJ, USA). Oleic acid was purchased from Wako pure chemicals (Osaka, Japan). Creatinine, uric acid and zinc nitrate hexahydrate were purchased from Acros Organics (New Jersey, USA). Urea was purchased from Riedel-de Haën (Seelze, Germany). Ethylene glycol was obtained from Scharlau Chemie (Barcelona, Spain). All the chemicals were reagent grade and used without further purification. Deionized Milli-Q water was used throughout the study.

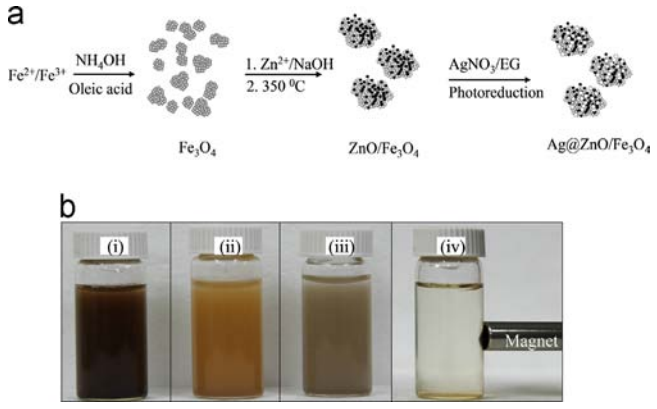

Fig. 1. (a) Schematic diagram for preparation of silver nanostructures-decorated ZnO/Fe_3O_4 composites. (b) Pictures for the corresponding synthesized Fe_3O_4 (i), ZnO/Fe_3O_4 composites (ii), Ag@ZnO/Fe_3O_4 composites (iii), Ag@ZnO/Fe_3O_4 composites assembled with permanent magnet (iv).

2.2. Preparation of ZnO/Fe_3O_4 composite

To prepare the composite, magnetic nanoparticles were first prepared by the coprecipitation method with some modification [36]. Briefly, 100 mL of 125 mM $FeSO_4$ and 62.5 mM of $Fe_2(SO_4)_3$ aqueous solutions were prepared. In this solution, 10 mL of ammonium hydroxide (28–30%, w/v) was added rapidly with vigorous stirring for 20 min to form magnetic precipitates. After addition of 4 mL of oleic acid, the precipitate was kept in an 85 °C water bath for 1.5 h. After cooling to room temperature, the magnetic precipitates were isolated from the solvent by magnetic decantation and washed several times by deionized water. These precipitates were further washed at least two times by ethanol.

In the synthesis of ZnO/Fe_3O_4 composites, 50 mg of Fe_3O_4 was soaked into a 50 mL solution of 45 mM zinc nitrate solution. After stirring and sonicating to form a well-dispersed solution, this mixture was dropped slowly into 50 mL of 90 mM NaOH solution at 70 °C with vigorous stirring within 40 min. This solution was kept in 70 °C water bath for 2 h and aged at room temperature for another 15 h to complete the reaction. The resulting composites were then separated with a magnet and washed with deionized water several times. After keeping in an 80 °C oven for 3 h, these particles were subsequently annealed at a temperature of 350 °C for 1 h. Once they are prepared, the composites were stored at room temperature and used for subsequent preparations of the SERS substrate by taking the required amount throughout the study.

2.3. Photochemical deposition of silver nanostructures on ZnO/Fe_3O_4 composite

To decorate silver nanostructures on the ZnO/Fe_3O_4 composite, 20 mg of the composite particles was taken and dispersed in 5 mL of $AgNO_3$ solution (in ethylene glycol) with the concentration ranging from 1 mM to 40 mM. The reaction mixture was then sonicated for 2 min to disperse the ZnO/Fe_3O_4 uniformly and placed into UV box for different lengths of irradiation times. The formed Ag@ZnO/Fe_3O_4 composite was cleaned with methanol or water using magnetic decantation and subsequently used as SERS substrate.

2.4. SERS measurements

To examine the performance of SERS activity of the prepared Ag@ZnO/Fe_3O_4 composites, 20 mg of the particles were soaked into 1 mL of 10 ppm methanolic *p*NTP solution and kept for 1 h. A Teflon protected cylindrical magnet (10 mm in diameter) was used to attract the Ag@ZnO/Fe_3O_4 composites. After being rinsed in methanol and air-dried, the composites were subsequently scanned by a Raman microscope as shown in Fig. 2. For detection of creatinine, 4 mg of the substrate was dispersed into 10 mL of an aqueous solution of creatinine, shaken for a while and kept for 30 min. Then, the particles were collected with a 3 mm iron bar attached with a permanent magnet. After being rinsed in water

and air-dried, the composites were subsequently scanned by a Raman microscope. On the other hand for an interference study, a final volume of 10 mL solution containing 50 mM NaOH and 1 μM creatinine alone or with 1 μM uric acid, 1 μM urea, and 10 μM NH_3 individually, was taken and the same procedure was applied as described above.

2.5. Instrumentation

The Raman spectra were measured by Triax 320 Raman system (Jobin-Yvon, Inc., Longjumeau, France), equipped with 632.8-nm He/Ne laser line as the excitation source (JDS Uniphase Corporation, Milpitas, CA) and a liquid-nitrogen cooled Ge array detector (Jobin-Yvon, Inc.). The laser power was 35 mW, and the exposure time was 0.2 s for measurement of pNTP and 5 s for creatinine unless and otherwise mentioned. Scanning electron microscopy (SEM) images and EDX spectra were obtained with JSM-6500F (JEOL, Ltd., Tokyo, Japan) field emission scanning electron microscope (FE-SEM) operating with an accelerating voltage of 10 kV. UV box (TS-UV, De-Yun, Ltd., Taipei, Taiwan) operating at 30 W with a wavelength range of 320–400 nm was used as a UV light source for photo-reduction process. X-ray diffraction (XRD) patterns were obtained on a D2 phaser XRD-300W powder diffractometer (Bruker, AXS GmbH, Karlsruhe, Germany) for a 2θ range of 20–80° at a scan rate of 0.05°/s using Cu Kα radiation at 40 kV and 100 mA.

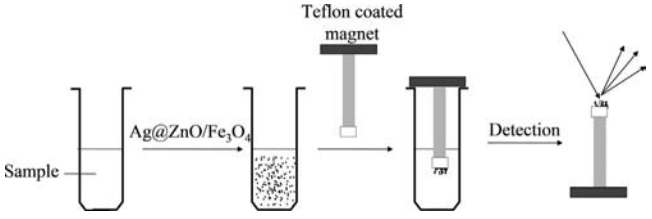

Fig. 2. Procedure and design used in detection of analytes.

3. Results and discussion

3.1. Basic studies for the prepared ZnO/Fe_3O_4 and Ag@ZnO/Fe_3O_4 composites

To characterize the prepared composites, samples of ZnO, Fe_3O_4, and the composites of ZnO/Fe_3O_4 and Ag@ZnO/Fe_3O_4 (growth in 20 mM silver nitrate/glycol solution for an irradiation time of 90 min) were first examined by SEM and powder X-ray diffraction (XRD). The SEM images of ZnO/Fe_3O_4 before decoration of Ag nanostructures are plotted in Fig. 3a with an enlargement in Fig. 3b. After being decorated with Ag nanostructures, the obtained image is plotted in Fig. 3c. Powder-like ZnO nanostructure with large elliptic ZnO crystals could be found in the SEM images shown in Fig. 3a and b. In the image of Ag@ZnO/Fe_3O_4, Ag nanocrystals were buried on the ZnO layers as can be seen in Fig. 3c. To verify the crystal structures, powder XRD was used and the obtained XRD patterns of the composites of ZnO/Fe_3O_4 and Ag@ZnO/Fe_3O_4 along with ZnO and Fe_3O_4 are plotted in Fig. 3d. Nine distinct diffraction peaks (Fig. 3d (i)) were observed for ZnO at $2\theta = 32.12°$, 34.76°, 36.58°, 47.85°, 56.88°, 63.22°, 66.92°, 68.29°, and 69.41° that are indexed to (1 0 0), (0 0 2), (1 0 1), (1 0 2), (1 1 0), (1 0 3), (2 0 0), (1 1 2) and (2 0 1) diffractions of ZnO crystals with a hexagonal wurtzite structure, indicating the formation of pure ZnO of high crystallinity [37]. The XRD diffraction peaks observed for isolated ZnO were also observed for ZnO/Fe_3O_4 composite (Fig. 3d (ii)) with additional peaks from Fe_3O_4 (see Fig. 3d (iii)) at diffraction angles of 30.6°, 35.98°, 43.64°, 54.04°, 57.54°, and 63.22° which can be marked with indices (2 2 0), (3 1 1), (4 0 0), (4 2 2), (5 1 1), and (4 4 0), respectively [38,39]. This confirms the formation of the composite with a core–shell-

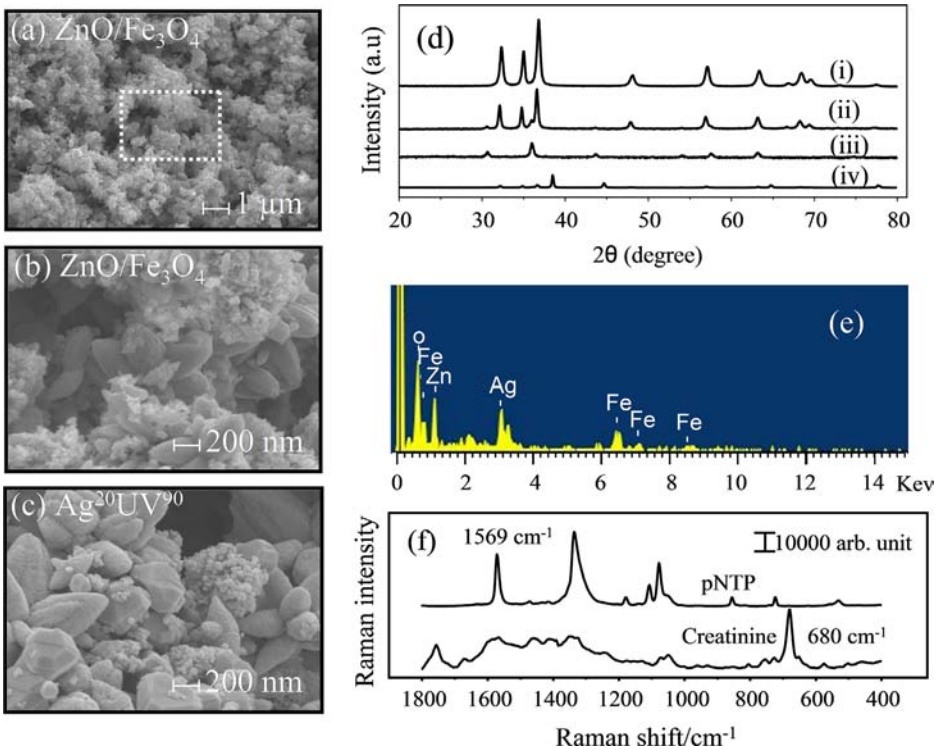

Fig. 3. (a) And (b) are SEM images of ZnO/Fe_3O_4 composites with different magnifications. (c) The SEM image of Ag@ZnO/Fe_3O_4 composites prepared in 20 mM of silver nitrate with an irradiation time of 90 min. (d) XRD pattern of ZnO (i), ZnO/Fe_3O_4 (ii), Fe_3O_4 (iii), and Ag@ZnO/Fe_3O_4 (iv). (e) EDX patterns of the Ag@ZnO/Fe_3O_4 composites. (f) The observed SERS spectra of *p*NTP and creatinine detected by Ag@ZnO/Fe_3O_4 composites.

like structure. These peaks – which are relatively weak but still observable in the Ag@ZnO/Fe_3O_4 composite structure with additional new strong four distinct diffraction peaks at diffraction angles of 38.2°, 44.3°, 64.7° and 77.5°, which correspond to (1 1 1), (2 0 0), (2 2 0) and (3 1 1) crystalline planes of cubic silver, respectively [39,40] – clearly show the dominance of silver nanocrystals in the composite (Fig. 3d (iv)). The formation of Ag@ZnO/Fe_3O_4 composites is further confirmed by the peaks observed in the EDX patterns that correspond to Ag, Fe, O, and Zn as shown in Fig. 3e. The SERS activity of the formed Ag@ZnO/Fe_3O_4 composites was also examined by probing with *p*NTP and aqueous creatinine solution as the typical observed SERS spectra are plotted in Fig. 3f. The detected SERS spectrum of *p*NTP shows three dominated bands located at 1338 cm^{-1} for NO_2 symmetrical stretching, 1569 cm^{-1} for phenyl ring stretching and 1079 cm^{-1} for C–H bending. Band features are in agreement with the literature [41]. In the detection of creatinine in aqueous solution as well as in urine sample, similar spectral features of creatinine were observed in the detected spectrum as can be seen in Fig. 3f. For instance, the prominent band at 680 cm^{-1} is observed, which could be attributed to the combinational mode of in-plane ring scissoring, C-NH_2 stretching, ring stretching, and C–O stretching [42]. Additional intense band is also observed at 1772 cm^{-1} that could be attributed to the combinational mode of C=O stretching, N–H in plane bending, and NH_2 wagging [42].

3.2. Effect of concentration of zinc nitrate to the SERS performance of Ag@ZnO/Fe_3O_4 composites

ZnO nanostructure plays an important role in the preparation of Ag@ZnO/Fe_3O_4 composites by photoreduction. As a semiconductor electronic structure, irradiation of ZnO with UV light promotes electrons from the valence band to the conduction band that could serve for the reduction of silver ions in the reaction mixture containing ZnO/Fe_3O_4 and $AgNO_3$ solution [35,43]. Concurrently, the valence band holes created would be used to oxidize ethylene glycol [44]. Meanwhile, ZnO prevents the inner Fe_3O_4 from oxidation to maintain the structure and thereby the magnetic property as indicated by Hong et al. [45]. By precipitating Zn ions on the surface of Fe_3O_4 nanoparticles under basic conditions, ZnO/Fe_3O_4 composites can be easily formed as characterized in the previous section. To optimize this chemical system, the concentrations of precursor zinc nitrate were varied to 15, 45, and 75 mM in the preparation of ZnO/Fe_3O_4 composites. The prepared composites were soaked in 5 mM silver nitrate/ethylene glycol solution to decorate Ag nanostructures with different UV irradiation times. After being probed with *p*NTP, the obtained Raman intensities were correlated with the UV irradiation time as shown in Fig. 4. An increase in concentration of ZnO resulted in an increment of the SERS intensities as weaker SERS intensities were observed using 15 mM zinc nitrate. This reveals that ZnO promotes efficiency in photoreduction of silver ions and the larger the amount of ZnO, the higher the SERS intensity. With an extensively long irradiation time, similar SERS intensities were observed for any of the examined concentrations of zinc nitrate. This may reveal that the amount of ZnO in the composites affects the photoreduction rate only or the magnetic nanoparticle can only uptake certain amount of ZnO. In any case, 45 mM zinc nitrate has been suggested to form the ZnO/Fe_3O_4 composites.

3.3. Optimization in preparation of Ag@ZnO/Fe_3O_4 composites for SERS applications

To optimize the parameters in the decoration of silver nanostructures to the ZnO/Fe_3O_4 composites by photoreduction, both UV irradiation time and concentration of silver nitrate in ethylene glycol were varied using ZnO/Fe_3O_4 composites prepared from 45 mM zinc nitrate for decoration of silver nanostructures. The concentration of silver nitrate was first varied up to 20 mM. With different irradiation times, the formed Ag@ZnO/Fe_3O_4 composites were probed with *p*NTP to observe the performances in SERS measurements as the results are plotted in Fig. 5a for the relationship between observed SERS intensities of *p*NTP and the irradiation times. As can be seen in this figure, maximal SERS intensities for each of the examined concentrates were located at around 90 min of irradiation time. This shows 90 min irradiation time could result in silver nanostructures of appropriate size and shape suitable for the higher SERS signals. Also, the higher the concentration of silver nitrate, the higher the SERS intensity obtained. The Ag@ZnO/Fe_3O_4 composites prepared with 20 mM of silver nitrate with different irradiation times were scanned by SEM as plotted in Fig. 5b–d. As can be shown in these photos, the Ag nanostructures in crystal forms could be seen. An elongation of the irradiation time increases the number and size of the Ag crystals. The diameters of the formed silver nanostructures with different irradiation times were estimated individually and fitted with Boltzman distribution function. Based on the images in Fig. 5b–d, the obtained diameters of the nanostructures are 146($\pm$ 90), 183 ($\pm$ 89), and 232($\pm$ 109) nm for an irradiation time of 30, 90, and 150 min, respectively. These values indicate that the increase of irradiation time results in an increase of particle size. Compared with the corresponding peak heights of *p*NTP in Fig. 5a, the particle diameter around 188 nm gives the highest intensity.

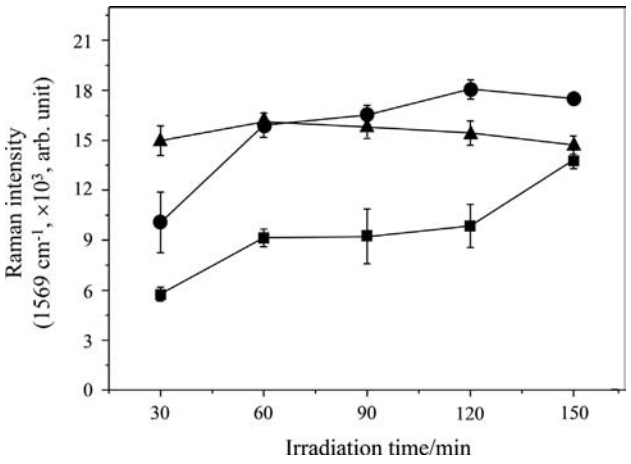

Fig. 4. Relationship between UV light irradiation time and SERS intensity of *p*NTP for the substrates obtained from the composites with a precursor Zn $(NO_3)_2$ solution of concentrations 15 mM (■), 45 mM (●), and 75 mM (▲).

To optimize the concentration of silver nitrate, an experiment was also carried out by keeping the irradiation time to 30 and 90 min but varying the concentration of silver nitrate. After being probed with *p*NTP, the observed SERS intensities are plotted in Fig. 6a. As can be seen in this figure, the optimal SERS intensity was obtained at 20 mM of silver nitrate regardless of irradiation time. Except for the data at 40 mM silver nitrate, the observed intensity patterns have a similar trend with a slightly higher SERS intensity with 90 min of irradiation time. Based on the small increases of the SERS intensities after elongating the irradiation time from 30 min to 90 min, the photoreactions may be limited by the concentration of silver nitrate. On the other hand, the concentration of silver ions in the solution may be extremely low to limit the growth of Ag nanostructures even under another 60 min of irradiation time. To verify this deduction, the Ag@ZnO/Fe_3O_4 composites were scanned with SEM and examples are plotted in Fig. 6b–d for composites prepared with 1, 5, and 40 mM of silver nitrate and 90 min of irradiation time. Clearly,

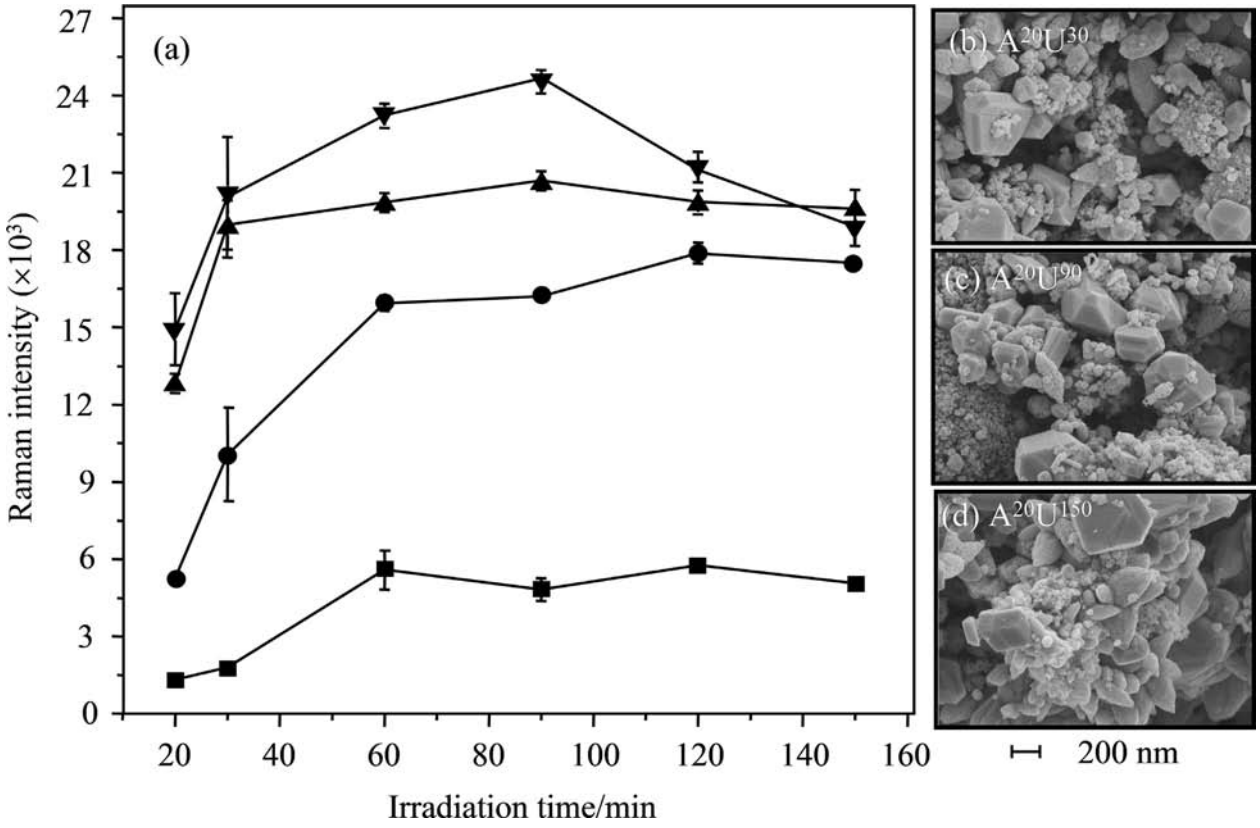

Fig. 5. (a) SERS intensity of *p*NTP showing the effect of UV irradiation time for a series of $AgNO_3$ solution of concentrations 1 mM (■), 5 mM (●), 10 mM (▲), and 20 mM (▼); (b)–(d) are SEM images of the composites prepared in 20 mM of silver nitrate with irradiation times of 30, 90 and 150 min, respectively.

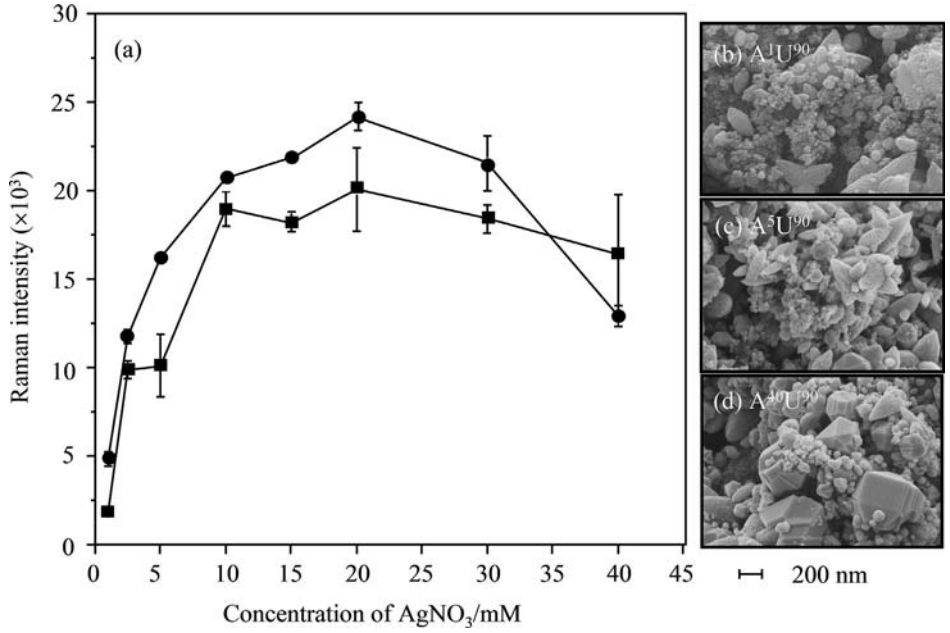

Fig. 6. (a) Relationships between SERS intensity of *p*NTP and concentration of silver nitrate under UV irradiation times of 30 min (■), and 90 min (●); and (b)–(d) are SEM images of the composites irradiated with 90 min of UV light with silver nitrate concentrations of 1, 5 and 40 mM, respectively.

not many Ag nanostructures could be observed in the composites prepared with a concentration lower than 5 mM. Furthermore, the supernatants after being separated from the magnetic composites were titrated with NaCl solution. Apparently, no white AgCl precipitate was observed for the supernatants with 90 min of irradiation time when silver nitrate concentration was lower than 20 mM. For silver nitrate concentrations higher than 30 mM, white precipitates were observed even under UV irradiation for 90 min. This reveals that silver ions are still available for a silver nitrate concentration higher than 20 mM. Therefore, photoreaction is concentration limited only under the condition that the concentration of silver nitrate is lower than 20 mM. With enough silver ions to grow the Ag crystals, a long photoreaction time can form a crystal size too big for SERS applications as the SERS intensity

starts to decrease when silver nitrate concentration was higher than 20 mM. Based on the observed images, the estimated diameters of the silver nanostructures are 132(± 32), 183(± 89), and 333(± 106) nm for silver nitrate concentrations of 5, 20, and 40 mM with an irradiation time of 90 min, respectively. The large particle formed by 40 mM of silver nitrate reduces the performance SERS measurements as only weak peak intensity of *p*NTP can be observed.

3.4. Evaluation of enhancement factor

The enhancement factor (EF) was calculated using the following equation:

$$EF = (I_{SERS}/I_{Raman})(N_{bulk}/N_{ads})$$

where I_{SERS} is the intensity of phenyl ring stretch of *p*NTP at 1569 cm^{-1} and I_{Raman} is the intensity for the same band in the Raman spectrum in 1% (w/v) methanoic solution of *p*NTP. The N_{bulk} is the number of *p*NTP in the laser beam path in measuring I_{Raman}, which was calculated from 1% (w/v) *p*NTP in the laser beam path (beam area × beam path). N_{ads} is the number of *p*NTP molecules in the cross section of the laser beam, which was deposited on Ag@ZnO/Fe_3O_4 with a surface density of 500 ng/cm^2. The calculated EF is found to be 9.1 (± 0.5) × 10^6.

3.5. Linearity, sensitivity and selectivity in detection of creatinine

To examine the feasibility of our prepared composites to determine creatinine in urine samples, Ag@ZnO/Fe_3O_4 prepared in 20 mM of silver nitrate with 90 min of irradiation was used. Creatinine was first dissolved in water to form standards to characterize the detection using our prepared composites. Referring to Fig. 3f, the pronounced and isolated band of creatinine located at 680 cm^{-1} was selected to characterize the analytical parameters in this study. By the same detection procedures, the obtained concentration–response curve is plotted in Fig. 7. As shown in this figure the SERS signals were found to increase sharply and linearly with the concentration of creatinine and reach a maximum around a concentration of 1 μM. After this point, the SERS signals remain almost similar regardless of the concentration of creatinine. This reveals that the active sites of Ag nanostructures are limited and easy to be occupied and saturated by creatinine molecules. The linear concentration range was found to be up to 1 μM with a slope and regression coefficient value of 24,628 (± 769) arb. unit/μM and 0.996, respectively. High reproducible results were obtained in these detections as the obtained average relative standard deviation in these measurements was only 3.75%. Based on 3 times the standard deviation in the blank test, the detection limit was found to be 24.8 nM. These values indicate that our prepared Ag@ZnO/Fe_3O_4 composites can be applied to detect creatinine sensitively. Compared with the reported detectable concentrations of creatinine by the literature SERS methods, which ranged from 4.4 μM to 216 μM [22–24], our method improves the sensitivity in the detection of creatinine significantly. This improvement is partially attributed to both the enrichment effect of magnetic materials and the large EF values of Ag nanostructures, which Au colloids cannot provide. Compared with detection limits by electrochemical methods, our proposed method is still better in sensitivity as the reported detection limits in electrochemical methods were around 100 μM [17,18]. This low sensitivity hinders the practical application of electrochemical methods for clinical monitoring.

For determination of creatinine in urine samples, the commonly co-existing species in urine such as uric acid, urea, and ammonia were first examined in an aqueous solution to observe their impacts on detections of creatinine. Mixtures containing 1 μM creatinine and one of the potential interfering species with a concentration of 1 μM were examined. No spectral features of urea and ammonia were observed in detection of these two species together with creatinine. However, intense bands from uric acid at 643 cm^{-1} and 1132 cm^{-1} that are attributed to skeletal ring deformation and C–O, C–C, C–N vibrations, respectively [46], in addition to the characteristics creatinine band at 680 cm^{-1} were observed when a mixture of 1 μM creatinine and 1 μM uric acid was examined as can be seen in Fig. 8c. To eliminate this strong interference from uric acid, the pH of the solution was adjusted to contain 50 mM NaOH. Under this high pH, each species in the solution should be fully deprotonated and the Ag nanostructures tend to carry a negative surface charge. On the other hand, all the species become neutral in charge with the exception of uric acid, which carries a negative charge. This can create charge repulsion force between Ag nanostructures and uric acid to terminate the spectral interference from this species. As can be seen from the spectra plotted in Fig. 8d, the spectral features of uric acid diminished under addition of NaOH. However, the efficiency to adsorb creatinine was also decreased slightly as the intensity of creatinine was decreased from 2.47 (± 0.11) × 10^4 to 1.69

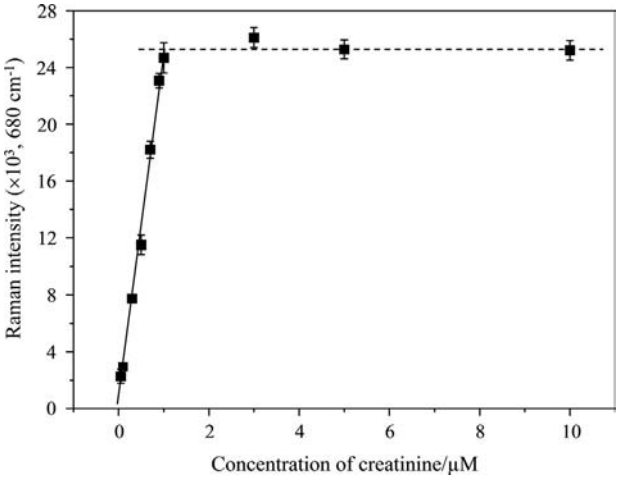

Fig. 7. Concentration–response profile of creatinine using Ag@ZnO/Fe_3O_4 composites prepared in 20 mM of silver nitrate with an irradiation time of 90 min.

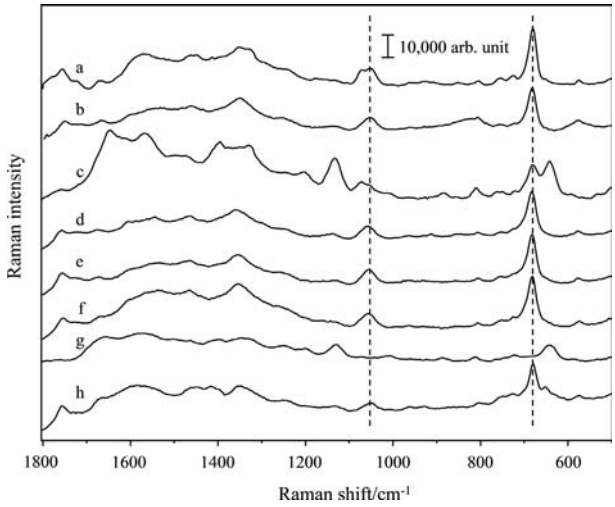

Fig. 8. Ag@ZnO/Fe_3O_4 composites in detection of aqueous solution of 1 μM creatinine (a), 1 μM creatinine with addition of 50 mM NaOH (b), 1 μM creatinine with addition of 1 μM uric acid (c), 1 μM creatinine with addition of 1 μM uric acid and 50 mM NaOH (d), 1 μM creatinine with addition of 1 μM urea and 50 mM NaOH (e), 1 μM creatinine with addition of 10 μM ammonia and 50 mM NaOH (f), urine sample with a dilution factor of 10^4 (g) and 10^4 time diluted urine sample with addition of 50 mM NaOH (h).

Table 1
SERS intensities of 1 μM creatinine detected under different conditions and the recoveries under different interferences. The concentrations of uric acid, urea, and ammonia in each solution were 1 μM, 1 μM and 10 μM, respectively. Solutions were adjusted with 50 mM NaOH.

Interference	SERS intensity ($\times 10^4$) (at 680 cm^{-1}, arb. unit)	Recovery (%)
None	1.68 ($\pm$ 0.04)	
Uric acid	1.71 ($\pm$ 0.11)	101.7 ($\pm$ 6.3)
Urea	1.82 ($\pm$ 0.10)	108.4 ($\pm$ 5.5)
Ammonia	1.90 ($\pm$ 0.05)	113.2 ($\pm$ 2.8)
Urea/uric acid/ammonia	1.86 ($\pm$ 0.04)	110.8 ($\pm$ 2.1)

($\pm$ 0.04) $\times 10^4$ when 50 mM NaOH was added. However, the interference from uric acid can be completely removed with a slight sacrifice on sensitivity in the detection of creatinine.

With the addition of NaOH, the detected SERS intensity of creatinine at 680 cm^{-1} was calculated and used to estimate the recovery in detection of creatinine under chemical interferences of the major species in urine samples as tabulated in Table 1. A recovery that is analytically acceptable was generally observed, indicating that our prepared Ag@/ZnO/Fe_3O_4 composites are selective in determination of creatinine.

3.6. Analysis of urine samples

To evaluate the substrate in real sample application, creatinine in urine sample was determined qualitatively and quantitatively. To decrease the matrix effect in the real samples, a dilution step was applied with a dilution factor of 10^4. The concentration of creatinine is also diluted. However, our prepared Ag@/ZnO/Fe_3O_4 composites are very sensitive in the detection of creatinine as the detection limit was around 25 nM. By diluting the sample under no addition of NaOH, no spectral feature of creatinine could be observed; instead the bands for uric acid are seen as shown in Fig. 8g. However, after addition of 50 mM NaOH into the diluted samples, feature bands of creatinine could be clearly seen as plotted in Fig. 8h. Based on these results, our proposed method can largely simplify the used pre-treatment steps in the literature methods. However, to obtain the concentration of creatinine in urine sample more accurately, 6-point standard addition method was used to further eliminate the effect of the matrix. By addition of creatinine in a concentration range up to 0.8 μM, the obtained regression line shows a regression coefficient of 0.996. Highly reproducible results were obtained in these detections as an average relative standard deviation of 3.05% was obtained. Based on the intercept and slope, the estimated concentration of the real urine sample is 9.75 ($\pm$ 0.67) mM after corrections by the dilution factor. This value agrees with the concentration of creatinine usually found in urine sample [47]. Compared with the literature SERS methods, the low enhancement effect of gold colloids used in the literature leads to weak band intensities so that only the vibrational band at 900 cm^{-1} [22,23] or non-specific vibrational band around 1400 cm^{-1} [24] can be used for quantitative purpose. On the other hand, the material prepared in this work is composed of silver nanostructures, which provide not only an enlargement in the enhancement but also a pronounced and unique band at 680 cm^{-1}. Hence, the prepared Ag@ZnO/Fe_3O_4 composites significantly increase the applicability in detection of creatinine in urine samples with a much better performance compared to the literature reported methods.

4. Conclusions

In this study, we successfully applied photochemical reduction method to prepare highly stable and sensitive multifunctional Ag@ZnO/Fe_3O_4 composites for SERS measurements. The prepared composite can be easily dispersed in the aqueous sample solution and interact rapidly with the analytes. The concentration effect acquired from the magnetic property of the composite helps decrease the detection limit via complete saturation of low concentration of analyte onto a minute amount of the composite. The dispersed composite in creatinine solution or urine sample is easily recovered with a magnet and SERS measurements provide a detection limit close to twentieth nanomolar. The selectivity of the substrate under several potential interfering species in aqueous solution and urine sample in detection of creatinine suggests its high capability as SERS substrate for biological samples analysis.

Acknowledgments

The authors thank the Ministry of Science and Technology of the Republic of China for their financial support for this work.

References

[1] T. Panasyuk-Delaney, V.M. Mirsky, O.S. Wolfbeis, Electroanalysis 14 (2002) 221–224.
[2] J.D. Jones, P.C. Burnett, Clin. Chem. 20 (1974) 1204–1212.
[3] P.C. Falcó, L.A.T. Genaro, S.M. Lloret, F.B. Gomez, A.S. Cabeza, C.M. Legua, Talanta 55 (2001) 1079–1089.
[4] S. Hallan, A. Asberg, M. Lindberg, H. Johnsen, Am. J. Kidney Dis. 44 (2004) 84–93.
[5] S.-L. Yan, P.-Z. Lin, M.-W. Hsiao, J. Chromatogr. Sci. 37 (1999) 45–50.
[6] F. Wei, S. Cheng, Y. Korin, E.F. Reed, D. Gjertson, C.-M. Ho, H.A. Gritsch, J. Veale, Anal. Chem. 84 (2012) 7933–7937.
[7] C.M. Gibson, D.S. Pinto, S.A. Murphy, D.A. Morrow, H.-P. Hobbach, S.D. Wiviott, R.P. Giugliano, C.P. Cannon, E.M. Antman, E. Braunwald, J. Am. Coll. Cardiol. 42 (2003) 1535–1543.
[8] J.A. Weber, A.P. Van Zanten, Clin. Chem. 37 (1991) 695–700.
[9] M.C. Gennaro, C. Abrigo, E. Marengo, C. Baldin, M.T. Martelleti, Analyst 120 (1995) 47–51.
[10] P. Boyne, B.A. Robinson, P. Murphy, M. McKay, Clin. Chem. 31 (1985) 1564–1565.
[11] B. Tombach, J. Schneider, F. Matzkies, R.M. Schaefer, G.C. Chemnitius, Clin. Chim. Acta 312 (2001) 129–134.
[12] R.T. Ambrose, D.F. Ketchum, J.W. Smith, Clin. Chem. 29 (1983) 256–259.
[13] T. Smith-Palmer, J. Chromatogr. B 781 (2002) 93–106.
[14] U. Lad, S. Khokhar, G.M. Kale, Anal. Chem. 80 (2008) 7910–7917.
[15] G.F. Khan, W. Wernet, Anal. Chim. Acta 351 (1997) 151–158.
[16] H. Thompson, G.A. Rechnitz, Anal. Chem. 46 (1974) 246–251.
[17] L. Campanella, F. Mazzei, M.P. Sammartino, M. Tomassetti, Bioelectrochem. Bioenerg. 23 (1990) 195–202.
[18] V. Razumas, J. Kanapienienė, T. Nylander, S. Engström, K. Larsson, Anal. Chim. Acta 289 (1994) 155–162.
[19] B. Sharma, R.R. Frontiea, A.-I. Henry, E. Ringe, R.P. Van Duyne, Mater. Today 15 (2012) 16–25.
[20] C.L. Haynes, A.D. McFarland, R.P. VanDuyne, Anal. Chem. 77 (2005) 338A–346A.
[21] K. Kneipp, H. Kneipp, I. Itzkan, R.R. Dasari, M.S. Feld, Chem. Rev. 99 (1999) 2957–2976.
[22] W.R. Premasiri, R.H. Clarke, M.E. Womble, Laser Surg. Med. 28 (2001) 330–334.
[23] H. Wang, N. Malvadkar, S. Koytek, J. Bylander, W.B. Reeves, M.C. Demirel, J. Biomed. Opt. 15 (2010) 027004.
[24] T.-L. Wang, H.K. Chiang, H.-H. Lu, F.-Y. Peng, Opt. Quant. Electron. 37 (2005) 1415–1422.
[25] R. Stosch, A. Henrion, D. Schiel, B. Güttler, Anal. Chem. 77 (2005) 7386–7392.
[26] R. Li, C. Han, Q.-W. Chen, RSC Adv. 3 (2013) 11715–11722.
[27] J. Yin, Y. Zang, C. Yue, Z. Wu, S. Wu, J. Li, Z. Wu, J. Mater. Chem. 22 (2012) 7902–7909.
[28] M. Gao, G. Xing, J. Yang, L. Yang, Y. Zhang, H. Liu, H. Fan, Y. Sui, B. Feng, Y. Sun, Z. Zhang, S. Liu, S. Li, H. Song, Microchim. Acta 179 (2012) 315–321.
[29] F. Xu, Y. Zhang, Y. Sun, Y. Shi, Z. Wen, Z. Li, J. Phys. Chem. C 115 (2011) 9977–9983.
[30] L. Sun, D. Zhao, Z. Zhang, B. Li, D. Shen, J. Mater. Chem. 21 (2011) 9674–9681.
[31] C. Cheng, B. Yan, S.M. Wong, X. Li, W. Zhou, T. Yu, Z. Shen, H. Yu, H.J. Fan, ACS Appl. Mater. Interfaces 2 (2010) 1824–1828.
[32] W. Song, Y. Wang, H. Hu, B. Zhao, J. Raman Spectrosc. 38 (2007) 1320–1325.
[33] P. Chen, L. Gu, X. Xue, Y. Song, L. Zhu, X. Cao, Mater. Chem. Phys. 122 (2010) 41–48.
[34] L. Yang, W. Ruan, X. Jiang, B. Zhao, W. Xu, J.R. Lombardi, J. Phys. Chem. C 113 (2009) 117–120.

[35] C. Pacholski, A. Kornowski, H. Weller, Angew. Chem. Int. Ed. 43 (2004) 4774–4777.
[36] Y. Tai, L. Wang, J. Gao, W.A. Amer, W. Ding, H. Yu, J. Colloid Interface Sci. 360 (2011) 731–738.
[37] J. Xia, A. Wang, X. Liu, Z. Su, Appl. Surf. Sci. 257 (2011) 9724–9732.
[38] K.-H. Choi, W.-S. Chae, E.-M. Kim, J.-H. Jun, J.-H. Jung, Y.-R. Kim, J.-S. Jung, IEEE Trans. Magn. 47 (2011) 3369–3372.
[39] S.F. Chin, K.S. Iyer, C.L. Raston, Cryst. Growth Des. 9 (2009) 2685–2689.
[40] R. He, X. Qian, J. Yin, Z. Zhu, J. Mater. Chem. 12 (2002) 3783–3786.
[41] B.O. Skadtchenko, R. Aroca, Spectrochim. Acta A 57 (2001) 1009–1016.
[42] J. Gao, Y. Hua, S. Li, Y. Zhang, X. Chen, Chem. Phys. 410 (2013) 81–89.
[43] T. Alammar, A.-V. Mudring, J. Mater. Sci. 44 (2009) 3218–3222.
[44] S. Chen, U. Nickelb, J. Chem. Soc. Faraday Trans. 92 (1996) 1555–1562.
[45] R.Y. Hong, S.Z. Zhang, G.Q. Di, H.Z. Li, Y. Zheng, J. Ding, D.G. Wei, Mater. Res. Bull. 43 (2008) 2457–2468.
[46] B.L. Goodall, A.M. Robinson, C.L. Brosseau, Phys. Chem. Chem. Phys. 15 (2013) 1382–1388.
[47] M.L. Bishop, J.L. Duben-Engelkirk, E.P. Fody, Clinical Chemistry, Principles, Procedures, Correlations, 4th ed., Lippincott Williams and Wilkins, New York (2000) 440 (Chapter 21).